Available online at www.sciencedirect.com

SCIENCE DIRECT

Virology 347 (2006) 379–391

VIROLOGY

www.elsevier.com/locate/yviro

Betanodavirus induces phosphatidylserine exposure and loss of mitochondrial membrane potential in secondary necrotic cells, both of which are blocked by bongkrekic acid

Shi-Ping Chen [a], Huey-Lang Yang [b], Guor Mour Her [c], Han-You Lin [b], Mei-Fen Jeng [d], Jen-Leih Wu [e], Jiann-Ruey Hong [a,*]

[a] *Laboratory of Molecular Virology and Biotechnology, Institute of Biotechnology, National Cheng-Kung University, Tainan 701, Taiwan, ROC*
[b] *Laboratory of Aquatic Animal Disease, Institute of Biotechnology, National Cheng-Kung University, Tainan 701, Taiwan, ROC*
[c] *Institute of Bioscience and Biotechnology, National Taiwan Ocean University, No. 2, Pei-Ning Road, Keelung 202-24, Taiwan, ROC*
[d] *Laboratory of Structural Biology, Institute of Biotechnology, National Cheng-Kung University, Tainan 701, Taiwan, ROC*
[e] *Laboratory of Marine Molecular Biology and Biotechnology, Institute of Cellular and Organismic Biology, Academia Sinica, Nankang, Taipei 115, Taiwan, ROC*

Received 31 August 2005; returned to author for revision 27 September 2005; accepted 29 November 2005
Available online 23 January 2006

Abstract

In this study, we show how the red spotted grouper nervous necrosis virus (RGNNV) causes loss of mitochondrial membrane potential and promotes host secondary apoptotic necrosis. RGNNV viral proteins such as protein α (42 kDa) and protein A (110 kDa) were quickly expressed between 12 h and 24 h postinfection (p.i.) in GL-av cells. Annexin V staining revealed that the NNV infection of GL-av cells induced phosphatidylserine (PS) externalization and development of bulb-like vesicles (bleb formation) at 24 h p.i. NNV infection also induced DNA fragmentation detectable by TUNEL assay between 12 h (8%) and 72 h (32%) p.i. Bongkrekic acid (1.6 μM; BKA) blocked permeability of the mitochondrial permeability transition pore, but cyclosporine A (CsA) did not block secondary necrosis. Finally, secondary necrotic cells were not engulfed by neighboring cells. Our data suggest that RGNNV induces apoptotic death via opening the mitochondrial permeability transition pore thereby triggering secondary necrosis in the mid-apoptotic phase.

Keywords: Nervous necrosis virus; Phosphatidylserine; Mitochondria; Bongkrekic acid; Phagocytosis

Introduction

Apoptosis is a process whereby individual cells of multicellular organisms commit suicide in response to a wide variety of stimuli (Wyllie, 1980). The genetically controlled and preprogrammed process eliminates cells during development to prevent redundancy. Alternatively, apoptosis may function as an emergency response following radiation damage, viral infection, or aberrant cell growth induced by oncogenes (Newton and Strasser, 1998). Apoptosis and necrosis are two stereotyped mechanisms by which nucleated eukaryotic cells die (Wyllie et al., 1980; Majno and Joris, 1995). Necrosis is considered to be a pathological reaction to major perturbations in the cellular environment such as anoxia (Herman et al., 1988), while apoptosis is considered to be a physiological process that preserves homeostasis by facilitating normal tissue turnover (Duvall and Wyllie, 1986; McConkey et al., 1989). The mechanisms leading to apoptosis are now better understood (Jeurissen et al., 1992; Shen and Shenk, 1995; Chen et al., 1997; Inoue et al., 1997; Hong and Wu, 2002) and appear to be different from one system to another. Understanding the biochemical and molecular mechanisms that control apoptosis may ultimately lead to novel therapeutic strategies.

Recently, several groups have reported that phosphatidylserine (PS) externalization during apoptosis can be sensitively measured using annexin V, a protein with a natural high affinity for this aminophospholipid. Annexin V has been used to show

* Corresponding author. Fax: +886 6 2766505.
E-mail address: jrhong@mail.ncku.edu.tw (J.-R. Hong).

0042-6822/$ - see front matter © 2005 Elsevier Inc. All rights reserved.
doi:10.1016/j.virol.2005.11.052

that PS export to the outer leaflet of the plasma membrane is an early and important event in apoptosis of cells from numerous lineages and that it is inhibited by overexpression of apoptosis repressor proteins such as Bcl-2 and v-Abl (Martin et al., 1995; Koopman et al., 1994). Interestingly, selective oxidation of phosphatidylserine (PSox) during apoptosis precedes externalization of PS in plasma membrane, a process that is essential for the engulfment of apoptotic cells. Tyuriana et al. (2004) proposed that PSox acts as a "non-enzymatic scramblase" and that it is likely to contribute to PS externalization.

Apoptosis is controlled at the mitochondrial level by the sequestration of apoptogenic proteins (such as cytochrome *c*, Smac/DIABLO, apoptosis inducing factor, and endonuclease G) in the mitochondrial intermembrane space, and the cytosolic release of these factors on exposure to proapoptotic signals (Wang, 2001; Madesh et al., 2002). Mitochondrial membrane permeabilization (MMP) allows cytosolic binding of caspase (the downstream activator of apoptosis) (Wang, 2001; Ferri and Kroemer, 2001). Also, proapoptotic signals mediated by cell death receptors are amplified through mitochondrial translocation of Bid, which in turn facilitates cytosolic release of cytochrome *c* and Smac/DIABLO, and caspase activation (Wang, 2001; Madesh et al., 2002; Kuwana, 1998). MMP can affect both the inner and outer mitochondrial membranes, and precedes the signs of necrotic or apoptotic cell death, including the apoptosis-specific activation of caspases (Zamzami and Kroemer, 2001). Adenine nucleotide translocase (ANT) plays a role in the exchange of ATP for ADP through the inner mitochondrial membrane, thus supplying the cytoplasm with ATP newly synthesized by oxidative phosphorylation. In a search for proapoptotic proteins, Bauer et al. (1999) identified the protein ANT1 as the main inducer of apoptosis. The overexpression of ANT1 produced rapid cell death, with a concomitant decrease in mitochondrial membrane potential ($\Delta\Psi m$) and an increase in nucleosomal DNA degradation. Since it was sensitive to a caspase inhibitor and to inhibitors of the mitochondrial permeability transition pore (MPTP) such as bongkrekic acid (BKA), apoptosis and the involvement of MPTP were indicated (Bauer et al., 1999). Hence, the mitochondrion is appreciated as a central integrator of prodeath stimuli, streamlining various types of proapoptic signals into a common caspase-dependent pathway (Ferri and Kroemer, 2001). But in the case of aquatic virus-induced host apoptotic cell death, little is known.

Nodaviruses are small, non-enveloped, spherical viruses with bipartite-positive-sense RNA genomes that are capped but not polyadenylated (Ball and Johnson, 1999). The family Nodaviridae contains two genera. Betanodaviruses predominantly infect fish, while alphanodaviruses mostly infect insects (Ball and Johnson, 1999; Schneemann et al., 1998; Van Regenmorted et al., 2000). Betanodaviruses infect a wide variety of larval and juvenile marine fish worldwide (Ball and Johnson, 1999), causing severe morbidity and mortality and significant economic losses to the aquaculture industry.

Despite their severe economic impact on the aquaculture industry, betanodaviruses are not well studied. Characterization of betanodavirus molecular regulation processes may help in elucidating the mechanism of viral pathogenesis and infection. In a previous study, greasy grouper (*Epinephelus tauvina*) nervous necrosis virus (GGNNV) of the Singapore strain was shown to induce apoptosis and activate the death effector enzyme caspase-3 in SB cells (Guo et al., 2003). In the present study, we demonstrate that the RGNNV induces apoptosis followed by secondary necrosis in GL-av cells and that loss of mitochondrial membrane potential in the mid-apoptotic stage may mediate this induction. This necrotic process was blocked by the mitochondrial permeability transition pore inhibitor BKA, which may also act by rescuing virus-infected cells.

Results

NNV viral protein expression early in the replication cycle

The larger genomic segment contains RNA1. RNA1 encodes protein A, which is part of the viral RNA-dependent RNA polymerase (RdRp) (Nagai and Nishizawa, 1999). In GL-av cells, protein A (MW, ca. 110 kDa) was expressed at 24 h post-RGNNV TN1 infection (p.i.) (as shown in Fig. 1, lane 4), and expression increased about 30% over a 24-h period between 30 h and 54 h p.i. (Fig. 1, lanes 5–8). The smaller genomic segment contains RNA2, which encodes a capsid protein named "protein α" (Nishizawa et al., 1995). In GL-av cells, a small amount of protein α (about 42 kDa) was rapidly expressed at 12 h p.i. (Fig. 1, lane 3); the amount expressed was larger between 24 h and 54 h p.i. (Fig. 1, lanes 4–8).

NNV induces exposure of PS at an early apoptotic stage

We used the GL-av cell line to test the feasibility of using annexin V-fluorescein labeling to detect early morphological

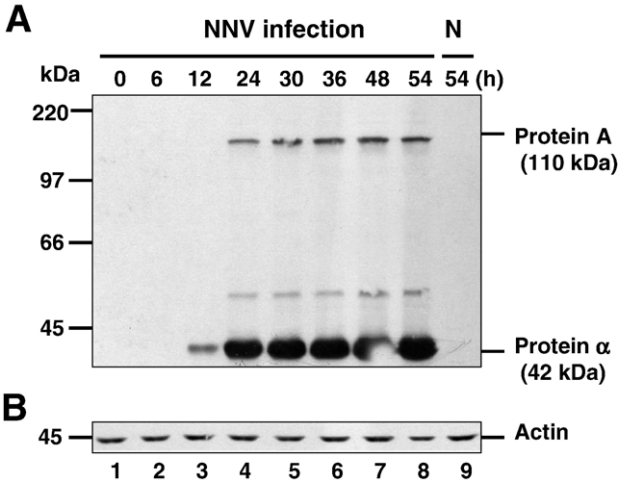

Fig. 1. Identification of RGNNV TN1 viral expression pattern in GL-av cells. (A) Expression of viral proteins in GL-av cells following incubation with RGNNV (m.o.i. 5) for 0, 6 h, 12 h, 24 h, 30 h, 48 h, and 54 h. Viral proteins such as NNV protein A and protein α were detected by Western blots, and the gels were immunoblotted with a polyclonal antibody to whole particle NNV. (B) The internal control in panel A was actin.

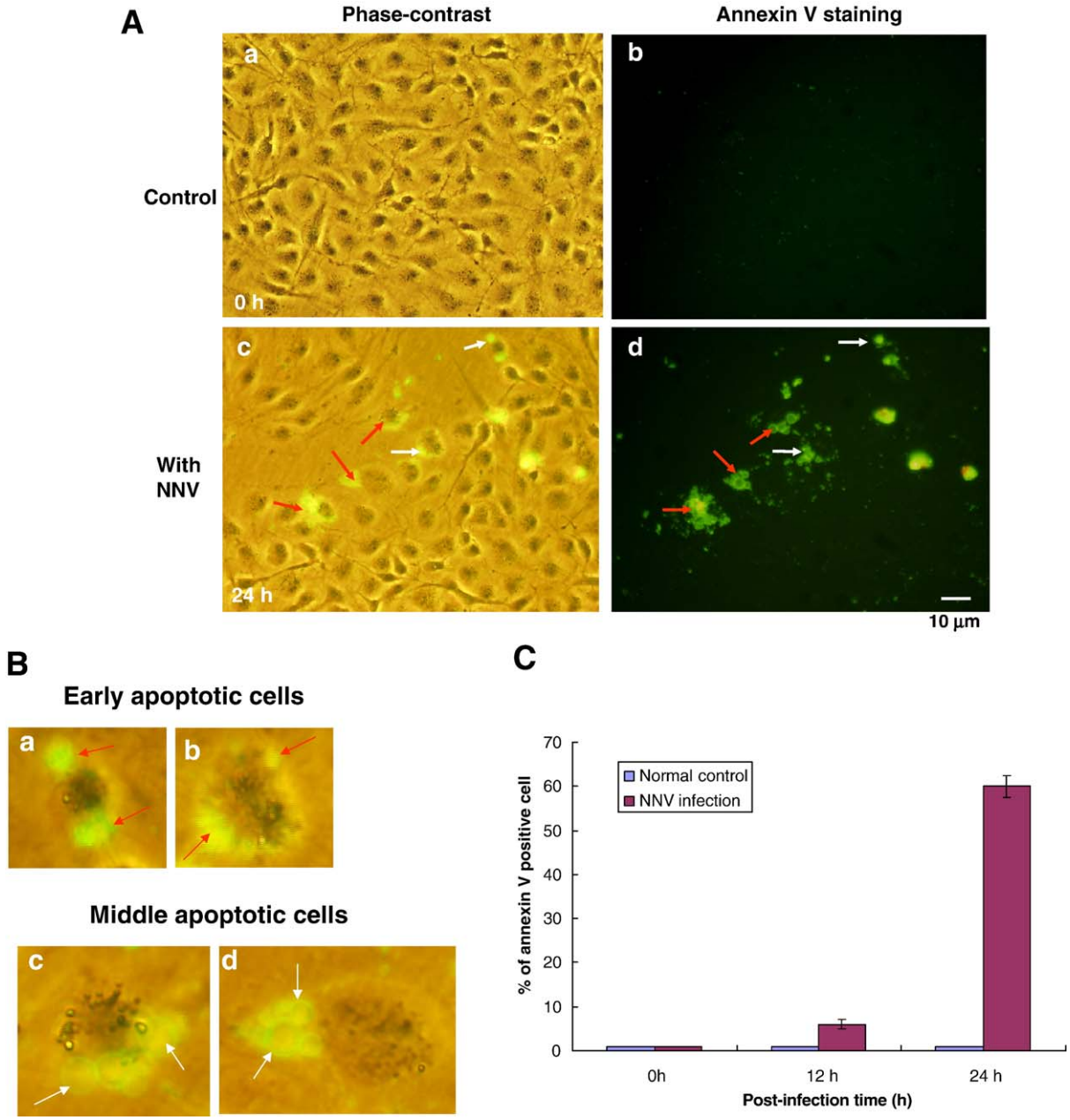

Fig. 2. Phase-contrast fluorescence image of RGNNV TN1-infected GL-av cells (m.o.i. 5). (A and B) Annexin V-labeled (fluorescing) early apoptotic (antiapoptotic bodies stained by annexin V; white arrows) and middle apoptotic cells (blebs stained by annexin V; red arrows) are present at 24 h p.i. (C) Percentage of annexin V-labeled uninfected or infected apoptotic GL-av cells at different time points p.i. (scale bar = 10 μm).

changes in apoptotic cells. Figs. 2A and B show the presence of early apoptotic cells during RGNNV TN1 infection under the conditions described above. Fig. 2A shows the externalization of PS from the inner membrane, different morphological patterns (Figs. 2A, c and d) associated with randomly exposed PS (Figs. 2B, a–c), and bleb formation in RGNNV-infected cells (Figs. 2B, d–e). Annexin V-positive cell assay (Fig. 2C) found that PS exposure is just minor at 12 h p.i. (6%) but is major at 24 h p.i. (60%) compared with normal control cells (0.5%). At all time points, the number of apoptotic-infected GL-av cells was significantly greater than the number of apoptotic mock-infected GL-av cells.

Visualization of the apoptotic and secondary necrotic morphological changes in GL-av cells

Terminal deoxynucleotidyl transferase (TdT)-dUTP labeling of uninfected and RGNNV TN1-infected GL-av cells showed that apoptosis, as indicated by the presence of double-stranded DNA fragments in situ, occurred in virus-infected cells at all times sampled (Figs. 3A: b, d, and f). Apoptotic nuclei were rarely observed in control GL-av cells (Figs. 3A: a, c, and e) (0.5%; $P < 0.05$). The concentration of apoptotic nuclei at 12 h, 24 h, 48 h, and 74 h p.i. was 8%, 12.5%, 25%, and 32% (as shown in Fig. 3B; all $P < 0.05$),

respectively. At all time points, the number of TUNEL-positive cells was significantly greater in RGNNV-infected GL-av cells than mock-infected GL-av cells. When the membrane integrity of GL-av cells was tested using acridine orange (AO) and ethidium bromide (EtBr) (dual dye labels used to identify apoptotic and postapoptotic necrosis cells), double-stained cells were observed at 72 h p.i. under phase-contrast microscopy. Fluorescence microscopy (Fig. 3C)

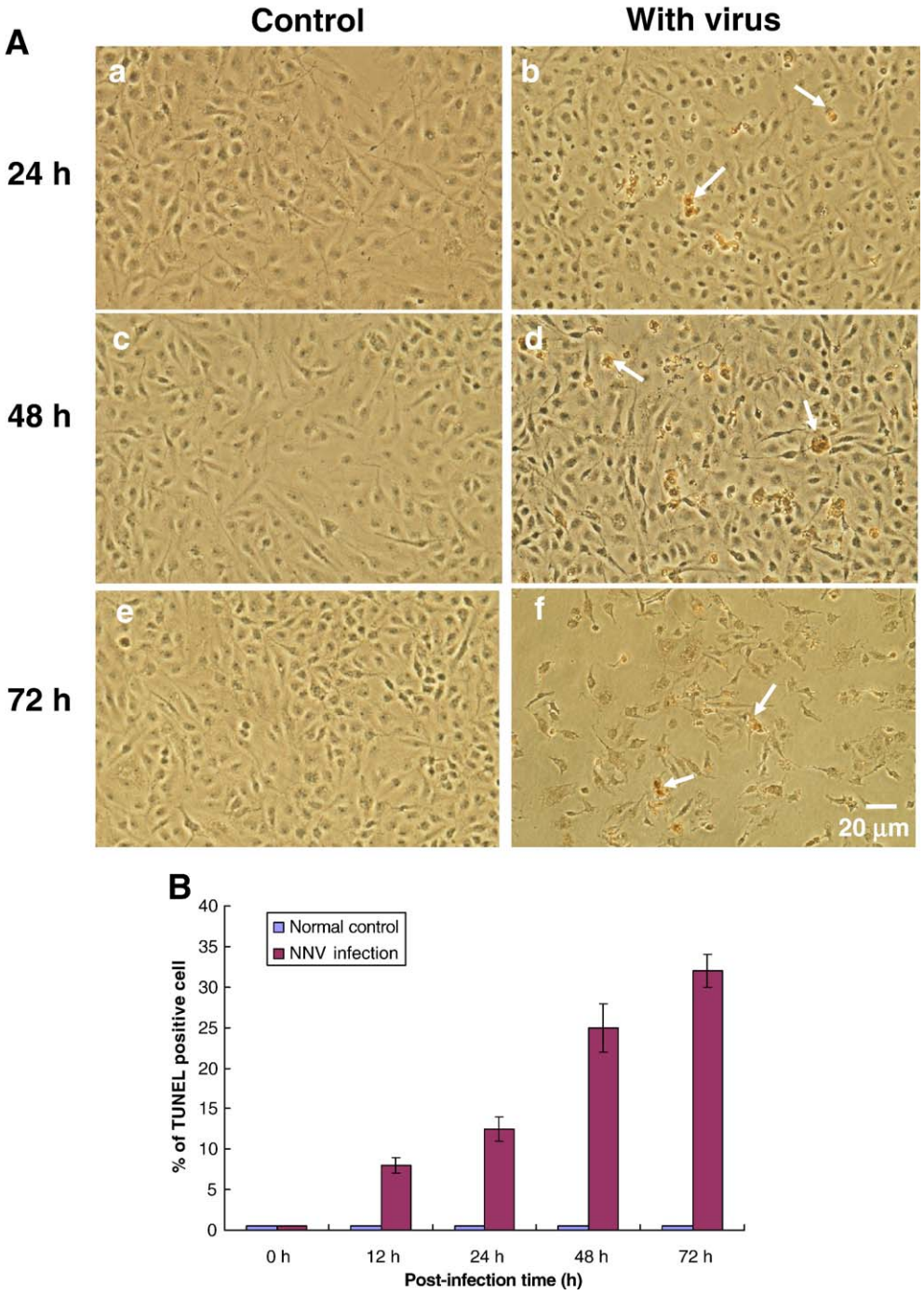

Fig. 3. Identification of GRNNV-induced apoptosis and postapoptotic necrosis in GL-av cells. (A) Infected and uninfected apoptotic GL-av cells (arrows) labeled with TdT-dUTP. Apoptotic nuclei are labeled with an orange red chromogen. (A: a, c, and e) Phase-contrast images of mock-infected GL-av cells (the normal control) showing TdT-dUTP-labeled apoptotic nuclei at 24 h, 48 h, and 72 h p.i., respectively. (A: b, d, and f) Phase-contrast images of infected GL-av cells (m.o.i. 5) showing TdT-dUTP-labeled apoptotic nuclei at 24 h, 48 h, and 72 h p.i., respectively (scale bar = 20 μm). (B) Percentage of uninfected or infected TdT-dUTP-labeled apoptotic GL-av cells at different time points p.i. (C) Phase-contrast fluorescence micrographs of acridine orange/ethidium bromide dye staining of uninfected GL-av cells at 72 h (a) and RGNNV-infected GL-av cells at 72 h (b; phase-contrast image only) and (c; phase-contrast fluorescence image) p.i. (C: a) Green fluorescence images of non-infected-GL-av cells, (C: b and c) mid-apoptotic cells (Ap; short arrow), and late apoptotic cells with postapoptotic necrotic cells (PN; long arrows), which are stained green, orange, and orange red.

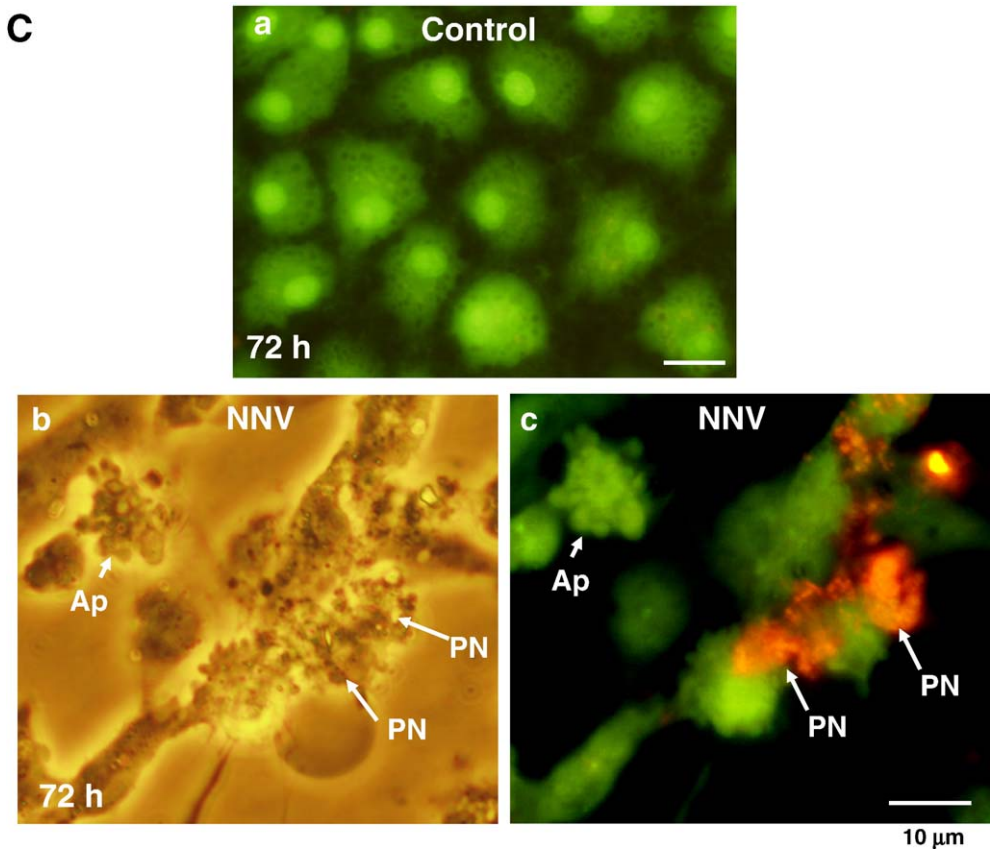

Fig. 3 (*continued*).

showed that the apoptotic (Ap) cells were AO-positive (Figs. 3C: b and c), the membrane integrity remained intact, and EtBr staining was negative. The postapoptotic necrotic (PN) cells were double positive (both green and orange) (Figs. 3C: b–c). Postapoptotic necrotic cells only weakly stained with AO, but because membrane integrity was lost, they showed positive staining with EtBr. At the same time, normal control GL-av cells were only stained with AO (Fig. 3C: a).

Secondary necrosis is correlated with loss of mitochondrial membrane potential in GL-av cells and is inhibited by the ANT-specific inhibitor BKA

To determine whether MPTP is involved in the cellular death induced by RGNNV infection, two known MPTP inhibitors, BKA and CsA, were used in inhibition tests of NNV-infected GL-av cells. GL-av cells were pretreated with BKA (1.6 μM) or CsA (16 μM) before RGNNV infection. BKA effectively blocked PS exposure in RGNNV-infected GL-av cells (Figs. 4C and D) (showing only slight staining for annexin V at 24 h p.i. in the presence of BKA and high percentage of annexin V-positive cells in its absence; Figs. 4A and B). CsA had no effect (data not shown). Then, the numbers of postapoptotic necrotic cells that showed bleb formation and PI positive staining were dramatically decreased by BKA treatment (compare Figs. 4F with E; arrows). BKA reduced the percentage of apoptotic cells from 75% to 36% and postapoptotic necrotic cells from 5% to 1.5% at 24 h p.i. (Fig. 4G). The number of Ab and PN was significantly greater in infected GL-av cells than in mock-infected GL-av cells.

Mitochondrial function was evaluated using MitoCapture Reagent (Apoptosis Detection, Mitochondria BioAssay™ Kit). The Mitocapture dye aggregates in the mitochondria of healthy cells and fluoresces red. In apoptotic cells, the dye cannot accumulate in mitochondria, remains as monomers in the cytoplasm, and fluoresces green. RGNNV-infected GL-av cells at 24 h p.i. quickly lost MPTP and the amount of red fluorescence decreased (Fig. 5A: f; arrows), and green fluorescence increased (Fig. 5A: e; arrows) in necrotic-like cells when compared to normal uninfected cells (Figs. 5A: b and c) and infected cells treated with BKA (Figs. 5A: h and i). Moreover (Fig. 5B), BKA (1.6 μM) effectively prevented the loss of MPTP at 24 h (2%) and 48 h p.i. (3.5%) when compared to untreated RGNNV-infected cells at 24 h (45%) and 48 h p.i. (10%) and to untreated uninfected cells at 24 h (1.5%) and 48 h (1.5%), respectively. At all time points p.i., the number of cells with MPTP loss was significantly greater in RGNNV-infected GL-av cells than mock-infected or BKA-pretreated infected GL-av cells. And finally, RGNNV-induced loss of MPTP corresponded to loss of cell viability (Fig. 5C). BKA enhanced cell viability of infected cells from 60% to 110% at 24 h p.i., and from 18% to 120% at 48 h p.i. The uninfected cell control also showed high viability at 24 h (120%) and 48 h (123%).

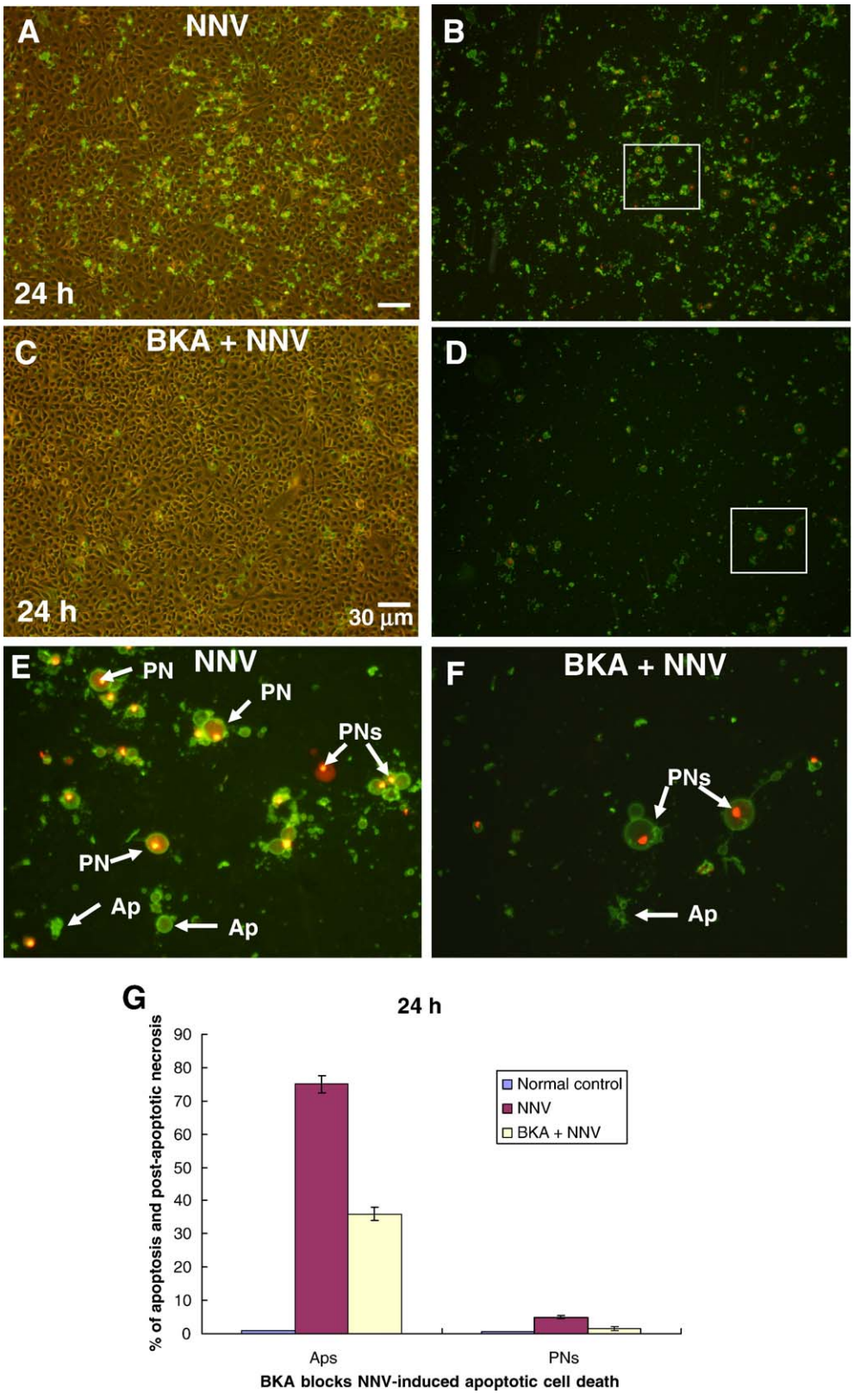

Fig. 4. BKA treatment can prevent either PS exposure or block secondary necrosis in RGNNV-infected (m.o.i. 5) GL-av cells at 24 h p.i. (A) Phase-contrast micrographs of annexin V-fluorescein labeling of infected GL-av cells. (C) Phase-contrast micrographs of annexin V-fluorescein labeling of BKA (1.6 μM)-pretreated infected GL-av cells. (B and E [enlargement of inset in panel B]) Fluorescent membrane-bound apoptotic bodies or blebs stained by annexin V on cells in panel A indicate the presence of apoptotic cells (Ab) and postapoptotic necrotic cells (PN), as indicated by arrows. (D and F [enlargement of inset from panel D]) Fluorescent membrane-bound apoptotic bodies or blebs stained by annexin V on cells in panel C indicate the presence of apoptotic cells (Ab) and postapoptotic necrotic cells (PN), as indicated by arrows (scale bar = 30 μm). (G) Percentage of annexin V-fluorescence-labeled apoptotic and postapoptotic necrotic GL-av cells with and without BKA treatment.

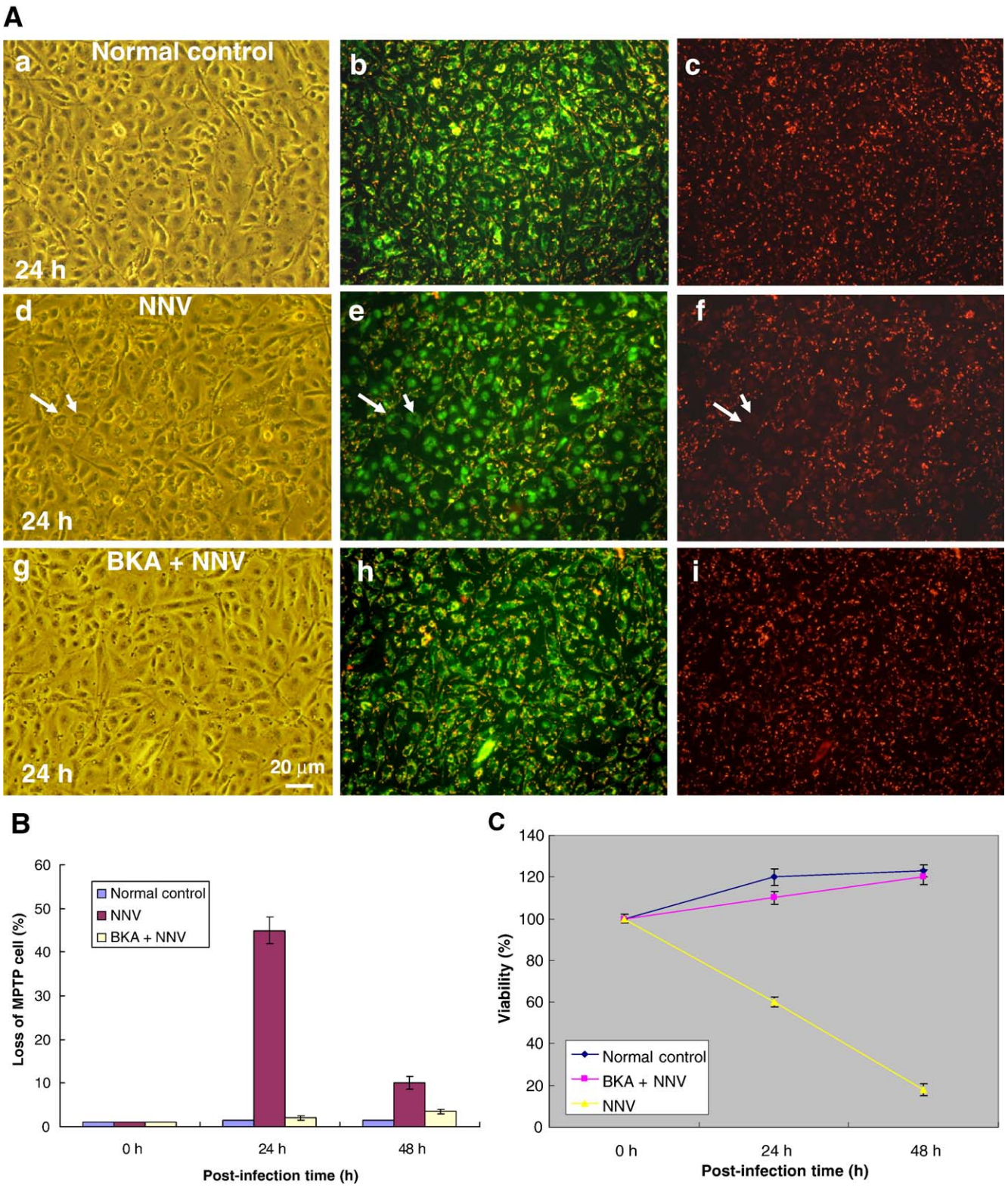

Fig. 5. BKA can block loss of mitochondrial membrane potential in GL-av cells infected with RGNNV (m.o.i. 5). Lipophilic cationic dye labeling shows that BKA (1.6 μM) pretreatment prevented the loss of MPTP in RGNNV-infected GL-av cells (arrows). The MPTP loss is demonstrated by either strong green fluorescence or loss of red fluorescence. (A, top panel: a–c) Phase-contrast fluorescence images of mock-infected GL-av cells (the normal control) stained with the lipophilic cationic dye. (A, middle panel: d–f) Phase-contrast fluorescence images of infected GL-av cells showing strong green fluorescence (A: e; arrows) and loss of red fluorescence (A: f; arrows). (A, bottom panel: g–i) Phase-contrast fluorescence images demonstrate that BKA treatment before infection of GL-av cells prevented loss of MPTP. The pattern of orange green fluorescence (A: h) and red fluorescence (A: i) retention is similar to that shown by normal control (uninfected) cells (scale bar = 20 μm). (B) Change in the percentage of dye-labeled RGNNV-infected GL-av cells (pretreated or not with BKA) indicates MPTP loss. (C) Trypan blue viability of RGNNV-infected GL-av cells (pretreated or not with BKA).

Neighboring cells failed to phagocytose secondary necrotic cells

RGNNV-infected cells underwent postapoptotic necrosis (secondary necrosis [SN]), but neighboring cells failed to engulf these secondary necrotic cells (Fig. 6). The SN cells were also aggregated and attached to the surface of normal cells (Figs. 6A and B) as evidenced by the orange color indicative of PS exposure (Fig. 6B, arrows) surrounding the strong green fluorescence of normal cells at 48 h p.i. TUNEL assay (Figs. 6B and D) yielded a similar result; TUNEL-positive individual cells (Fig. 6C) and clustered cells (Fig. 6D; arrows) attached to normal cell surfaces were noted. When overexpressed, enhanced green fluorescent protein (EGFP; 36 h posttransfection [p.t.]) induced apoptosis (Figs. 6E: b and c) and apoptotic body formation in a small number of cells. The figure showing GL-av cells engulfing these apoptotic bodies (Figs. 6E: d and e, arrows) at 48 h p.t. is included as a positive control.

Discussion

RGNNV-infected fish lie on their sides, float belly up, or swim abnormally (such as swimming in circles or to the right). Histopathological changes in infected fish include extensive cellular vacuolation and neuronal degeneration by necrosis in the central nervous system and retina (Delsert et al., 1997; Grotmol et al., 1999; Mori et al., 1992; Nakai et al., 1994). Although betanodavirus infection is known to induce neuronal degeneration and is correlated with abnormal swimming, this effect remains an interesting problem for possible investigation in the future. In the present study, the process of switching from early apoptosis to necrosis was investigated to explain how RGNNV TN1 infection damages host cells.

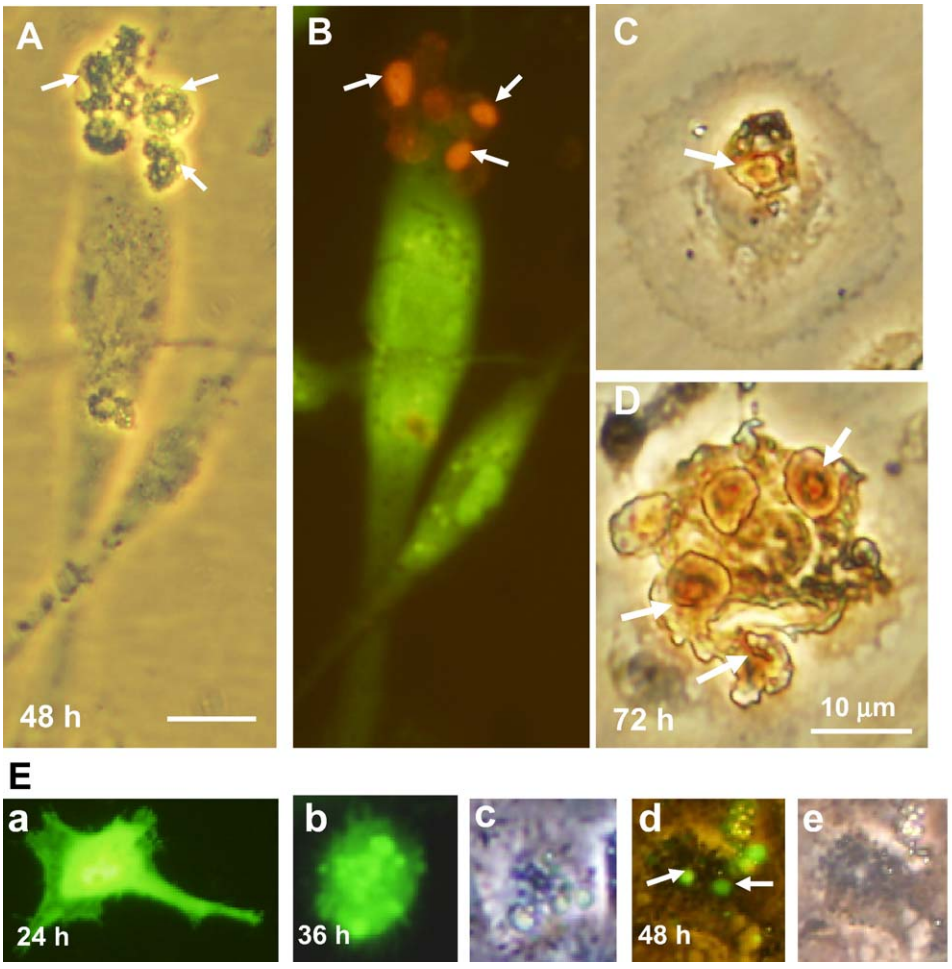

Fig. 6. Phase-contrast micrographs demonstrating the failure of neighboring cells to engulf postapoptotic GL-av cells. GL-av cells were infected with RGNNV (m.o.i. 5) and stained with acridine orange/ethidium bromide dyes (A and B) for 48 h p.i. and with TdT-dUTP (C and D) for 72 h p.i. (A) Phase-contrast micrograph of acridine orange/ethidium bromide stained RGNNV-infected GL-av cells showing clustering of postapoptotic necrotic cells (arrows) and attachment to the plasma membrane of neighboring cells. (B) The fluorescence images of postapoptotic necrotic cells (stained orange red) are strongly labeled with both dyes (arrows). (C and D) Phase-contrast image of post apoptotic necrotic GL-av cells infected with RGNNV (m.o.i. 5) at 72 h p.i. shows clustering of TdT-dUTP-labeled apoptotic nuclei (arrows) and their attachment to the surface of neighboring cells (scale bar = 10 μm). (E) GL-av cells engulfed the apoptotic bodies containing EGFP. (E: a) Phase-contrast fluorescence image of GL-av cells transfected with EGFP plasmid 24 h p.t. (E: b and c) Phase-contrast and fluorescence image of GL-av cells transfected with EGFP plasmid at 36 h p.t. show that EGFP can induce apoptotic death of GL-av cells. (E: d and e) Phase-contrast and fluorescence image of GL-av cells engulfing the EGFP-induced apoptotic bodies (arrows) at 48 h p.t.

The features of necrotic and apoptotic cell death are well described and reviewed elsewhere (Kerr et al., 1972; Jaeschke and Lemasters, 2003). Apoptosis is a morphologically distinct form of cell death that spontaneously occurs in many different tissues under various conditions (Falcieri et al., 1994). It occurs in distantly separated cells and progresses very rapidly, never causing exudative inflammation in tissues. No cell hydration takes place, but nuclear (see Fig. 3A: d, the TUNEL-positive cell) and cytoplasmic condensation (Fig. 3C: c; the Ap cell) can appear, followed by the formation of numerous membrane-bound cell fragments termed "apoptotic bodies." In contrast to necrosis, the nuclear organization is completely lost (see Fig. 3C: c, the PN cell). Surprisingly, both cytoplasmic and organellar components remain intact for some time unless the cell undergoes secondary necrosis (see Fig. 3C: c, the PN cell). This penultimate event is due to plasma membrane rupture and consequently the abrupt loss of the plasma membrane permeability barrier (Nieminen et al., 1988; Hong et al., 1998). Secondary necrosis, sometimes called "postapoptotic necrosis," occurs only in the final apoptotic stage (Falcieri et al., 1994).

The present results indicate that RGNNV infection of the grouper liver cell line (GL-av) induces early apoptotic changes (partial detachment (Figs. 2B: a–b) and PS exposure (Figs. 2B: a–b) at 12 h p.i.), mid-apoptotic changes (further cell detachment, bleb formation on the plasma membrane (Figs. 2B: c–d), DNA fragmentation (Figs. 3A and B), and loss of MPTP (Figs. 5A and B) at 12–24 h p.i.), postapoptotic necrotic changes (abnormal chromatin-condensation (Figs. 3C: b and c) and loss of the plasma membrane permeability barrier (Figs. 3C: b and c) at 24–48 h p.i.), and finally necrosis.

A recently discovered family of proteins, the annexins, has been found to have a high affinity for aminophospholipids in the presence of Ca^{2+} (Andree et al., 1990; Raynal and Pollard, 1994). A member of this family, annexin V, has been shown by several groups to preferentially bind PS (Andree et al., 1990; Tait et al., 1989; Thiagarajan and Tait, 1990). Thus, annexin V provides a convenient tool for determining directly whether changes in membrane PS distribution occur as a general feature of apoptosis and measuring the kinetics of these changes on a single-cell basis. Our study found that RGNNV-induced apoptosis and postapoptotic necrosis (Figs. 2A: d and 4E) were accompanied by increased annexin V-binding (dramatic changes in PS distribution) to the plasma membrane. The observations of Fadok et al. (1992) suggest that apoptotic lymphocytes lose membrane phospholipids asymmetry and expose PS on the outer leaflet of the plasma membrane. In early mid-apoptotic GL-av cells, we found that PS exposure occurred rapidly on the outer leaflet of the plasma membrane and that bulb-like vesicles developed (Figs. 2B: d–e and 4E). These events were very specific, but their function still remains to be examined.

Mitochondrial membrane permeabilization (MMP), which can affect both the inner and outer mitochondrial membranes, precedes the signs of necrotic or apoptotic cell death (Lemasters, 1999; Marzo et al., 1998; Narita et al., 1998; Shimizu et al., 2001; Kim et al., 2003). MMP is mainly controlled by porins (voltage-dependent anion channel [VDAC] proteins) and adenine nucleotide translocase (ANT), two of the most abundant proteins of the outer and inner mitochondrial membranes. These have also been shown to interact with the Bcl-2 family of proteins and to mediate mitochondrial damage during apoptosis (Marzo et al., 1998; Narita et al., 1998; Shimizu et al., 1999).

Many reports show that apoptosis correlates with signs of a permeability transition, such as loss of mitochondrial transmembrane potential ($\Delta\Psi m$), and that induction of a permeability transition is enough to trigger cell death (Compton, 1999; Kroemer et al., 1998). Some potent drugs inhibiting this permeability transition can prevent cell death (Compton, 1999; Kroemer et al., 1998). For example, cyclosporine A (CsA), which is a non-immunosuppressive derivative that acts on cyclophilin D can inhibit apoptosis induced in vivo by brain trauma (Sullivan et al., 1999) and ischemia reperfusion damage (Compton, 1999). Moreover, bongkreic acid (BKA), an ANT ligand that inhibits the permeability transition pore complex (PTPC), prevents apoptosis stimulated by diverse stimuli such as glucocorticoids (in thymocytes) (Kroemer et al., 1998), excitotoxins (in neurons) (Budd et al., 2000), and tumor necrosis factor (in hepatocytes) (Tafani et al., 2000). However, such pharmacological inhibitors are not universally cytoprotective, implying that permeabilization of the mitochondrial membrane may involve individual PTPC components (for example, the VDAC without the ANT/cyclophilin D) or occur in a completely PTPC-independent fashion. Interestingly, in our grouper liver cell line, we found that BKA prevented up to 40% of NNV-induced apoptosis (Figs. 4B, D, and G) and eventually blocked postapoptotic necrosis in the mid-apoptotic stage up to 3.5% (reducing it from 5% to 1.5%) at 24 h p.i. (Figs. 4E, F and G). However, the cyclophilin D inhibitor CsA had no effect because cyclophilin D is located in the inner membrane (IMM) compartment and acts only in conjunction with ANT. Moreover, BKA inhibited the loss of the MPTP by up to 43% at 24 h p.i. (Figs. 5A: g, h, i, and C), and enhanced the viability of infected cells by up to 50% (Fig. 5D; 24 h p.i.) and 112% (48 h p.i.), indicating that the loss of MPTP is strongly correlated with the infection-induced transition to postapoptotic necrosis from early apoptosis. On the other hand, zebrafish Bcl-x_L blocked RGNNV-induced loss of MPTP (data not shown). Whether host cell death (which is also correlated to loss of MPTP and cytochrome *c* release) occurs via a caspase-dependent or caspase-independent pathway (Chipuk and Green, 2005) in this system remains to be discovered. The fact that some alphanodaviruses such as FHV (Miller et al., 2001) and NoV replicate in mitochondria (Garzon et al., 1990) or on the outer mitochondrial membrane (Miller et al., 2001) raises the question of whether apoptosis and viral replication on mitochondrial membranes are related. Our data showed that BKA, by blocking the loss of MPTP in RGNNV-infected cells, effected a 2 log (48 h p.i.) and 1.5 log (72 h p.i.) reduction in viral titer (data not shown). Though localization of the RNA-dependent RNA polymerase (RdRp) of the betanodavirus GGNNV (Guo et al., 2004) in mitochondrial membrane has been shown, there is as yet no evidence linking RdRp to host

cell apoptotic cell death. On the other hand, the capsid protein of GGNNV has been shown to induce apoptosis in SB cells (Guo et al., 2003), but we found that the RGNNV capsid protein accumulates largely in the nucleus of GL-av cells. Possibly, RGNNV induces apoptosis when its RNA replication machinery in mitochondrial membranes is re-targeted to the ER as described by Miller et al. (2003). On this point, we have some evidence to show that RGNNV-induced host cell death requires new protein synthesis, but whether a viral or host protein is essential is still unknown.

The apoptotic pathway and the engulfment process are part of a continuum that helps ensure the non-inflammatory nature of this death paradigm. Phagocytes recognize the surface of the dying cell most likely through an "eat me" signal. In mammalian systems, the best characterized "eat me" signal is phosphatidylserine displayed on the plasma membrane of dying cells (Savill and Fadok, 2000). Evidence has been marshaled for the participation of multiple engulfment receptors including CD91, CD14, CD36, and $\alpha v\beta_3$ integrin, as well as the phosphatidylserine receptor (Fadok et al., 2000; Hong et al., 2004). Studies in mammals have highlighted the importance or proper disposal of corpses by phagocytic cells (Savill and Fadok, 2000). In addition to engulfment of apoptotic cells, macrophages are important regulators of proinflammatory responses by releasing cytokines such as TNFα. While proinflammatory factors are necessary in the immune reaction to infection, their suppression during apoptotic corpse clearance is essential.

We found that PS exposure is minor (6%) in early apoptotic stage at 12 h p.i. (Fig. 2C), and increases quickly (to 60%) in the mid-apoptotic stage at 24 h p.i. (Fig. 2C). In this stage, some cells enter the postapoptotic necrotic phase (5%; Fig. 4G). Late apoptotic GL-av cells that have also undergone postapoptotic necrosis (secondary necrosis) and failed to be engulfed by neighboring cells (Figs. 6A–D) may have lost PS molecules and may have no PS receptors. But this issue remains unresolved.

In a previous study, Guo et al. (2003) found that greasy grouper (*E. tauvina*) nervous necrosis virus (GGNNV) of the Singapore strain can induce apoptosis possibly by activating caspase-3 in SB cells (Guo et al., 2003). On the other hand, in our system, cell death was not consistently associated with caspase-8, -9, and -3 activation, suggesting involvement of an alternative mechanism such as caspase-independent cell death (CICD) (Chipuk and Green, 2005; Kroemer and Martin, 2005).

In summary (see Fig. 7), NNV TN1 kills cells by inducing apoptosis, causing loss of mitochondrial membrane potential in the mid-apoptotic stage. This loss may contribute to the triggering of secondary necrosis in the late apoptotic stage

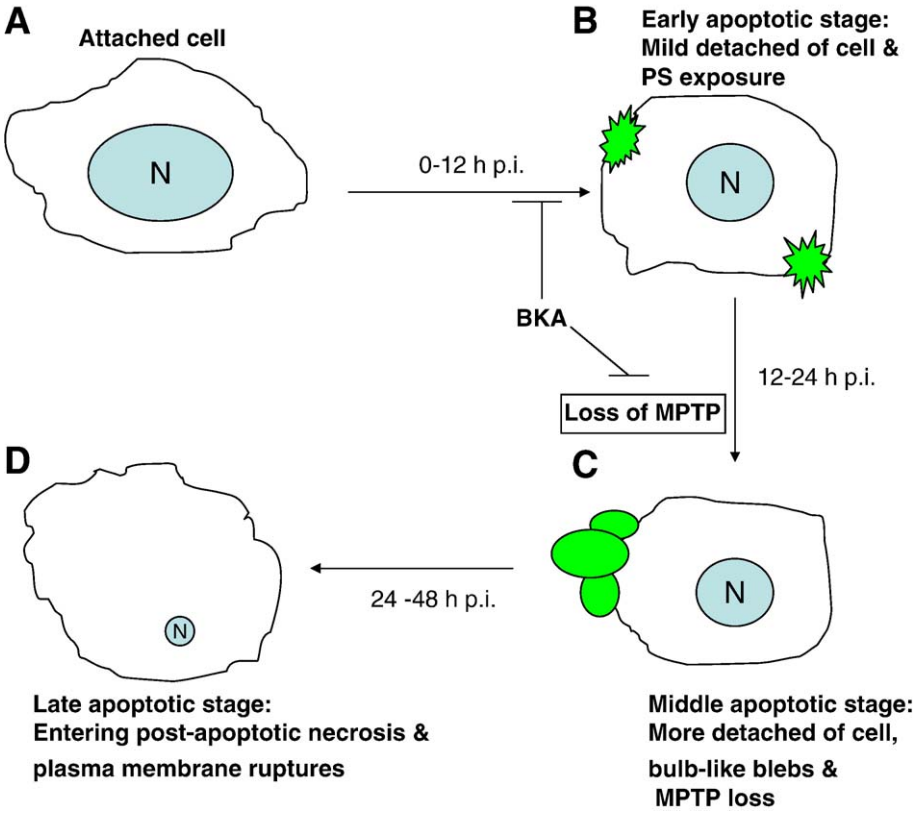

Fig. 7. Diagram illustrating the morphological changes and molecular events induced in fish cells by RGNNV TN1 infection. (A) Normal attached cell. (B) In the early stage of apoptosis (A to B, 0–12 h p.i.), the cell partially detaches from the extracellular matrix and PS is exposed. (C) In the middle stage (12– 24 h p.i.), the apoptotic cell is more detached from the extracellular matrix, blebs form from the plasma membrane, DNA fragmentation occurs, and MPTP loss, which can be blocked by BKA, occurs. Finally, in the late stage of apoptosis (24–48 h p.i.), either nuclear membrane integrity is disrupted or a postapoptotic necrosis (secondary necrosis) occurs, during which the plasma membrane is ruptured causing loss of the plasma membrane permeability barrier.

and the failure of neighboring cells to engulf secondary necrotic cells. In addition, secondary necrotic cell death is also prevented by the ANT inhibitor BKA but not by the cyclophilin D inhibitor CsA. BKA may be a therapeutic agent for this viral infection.

Materials and methods

Cell culture and reagents

The grouper liver cell line (GL-av) was subcloned from the grouper liver cell line (GL-a) obtained from Dr. Lang (Institute of Biotechnology, National Cheng-Kung University, Taiwan, ROC). The cell line was grown at 28 °C in Leibovitz's L-15 medium (GibcoBRL, Gaithersburg, MD, USA) supplemented with 5% fetal bovine serum and 25 μg/ml of gentamycin. Annexin V-FLUOS Kit and In Situ Cell Death Detection Kit were purchased from Roche GmbH (Mannheim, Germany). Bongkrekic acid (BKA), cyclosporine A (CsA), and acridine orange (AO) were all purchased from Sigma Chemical Co. (St. Louis, MO, USA). Anti-NNV particle polyclonal antibody was obtained from Dr. Jen-Leih Wu's Laboratory. ECL Western blotting detection system kit was purchased from Amersham (Piscataway, NJ, USA). Apoptosis Detection, Mitochondria BioAssay™ Kit was purchased from USBiological (Jomar Diagnostics Pty. Ltd., Stepney, SA, Australia).

Virus

Naturally infected red grouper larvae were collected in 2002 in the Tainan prefecture and were the source of red spotted grouper nervous necrosis virus (RGNNV *T*ainan *N*o. *1*; RGNNV TN1) used to infect GL-av cells. The virus was purified as described by Mori et al. (1992) and stored at −80 °C.

Western blot analysis

The GL-av cells were cultured by seeding 10^5 cells/ml in a 60-mm Petri dish for 20 h prior to rinsing the monolayers twice with phosphate-buffered saline (PBS). Cells were infected at a multiplicity of infection (m.o.i.) of 5 with RGNNV TN1 strain (previously propagated and titrated in GF-1 cells where the virus was found to have a $TCID_{50}$ of 10^8/0.1 ml), and infected cells were incubated for 0, 6 h, 12 h, 24 h, 30 h, 36 h, 48 h, and 54 h. At the end of each incubation time, the culture medium was aspirated and the cells were washed with PBS and then lysed in 0.3 ml of lysis buffer (10 mM Tris base, 20% glycerol, 10 mM sodium dodecyl sulfate [SDS], and 2% β-mercaptoethanol [β-ME], pH 6.8). An aliquot of the lysate was used for the separation of proteins by SDS-polyacrylamide gel electrophoresis (Laemmli, 1970). The gels were subjected to immunoblotting (Kain et al., 1994). Blots were incubated with a 1:3000 dilution of rabbit anti-RGNNV polyclonal antibody and subsequently a 1:7500 dilution of a peroxidase-labeled goat anti-rabbit conjugate (Amersham Biosciences, Piscataway, NJ, USA). Binding was detected by chemiluminescence and captured on Kodak XAR-5 films (Eastman Kodak, Rochester, NY, USA).

Annexin V-FLUOS staining

An analysis of PS on the outer leaflet of apoptotic cell membranes was performed using annexin V-fluorescein and propidium iodide (PI) to differentiate apoptotic from necrotic cells. At the end of various incubation times (0, 12 h, and 24 h), each sample was removed from the medium and washed with PBS, and then cells were incubated with 100 μl of staining solution (annexin V-fluorescein in a HEPES buffer containing PI; Boehringer-Mannheim, Mannheim, Germany) for 10–15 min. Evaluation was by fluorescence microscopy using a 488-nm excitation and 515-nm long-pass filter for detection (Hong et al., 1998).

TdT-dUTP labeling

For TdT-dUTP labeling, GL-av cells (10^5 cells/0.1 ml) were seeded on 35-mm Petri dishes (Nunc) at 28 °C for 20 h. The negative control dishes received 2 ml of 5% FBS L-15 medium. The two treatment groups were then incubated at 28 °C for 0, 12 h, 24 h, 48 h, and 72 h, after which the cells were harvested from the medium, washed with PBS, mounted on slides, and then fixed with a freshly prepared paraformaldehyde solution (4% in PBS, pH 7.4) for 30 min at room temperature. Slides were washed with PBS and incubated with blocking solution (0.3% H_2O_2 in methanol) for 30 min at room temperature.

Petri dishes were rinsed with PBS, incubated in permeabilization solution (0.1% Triton X-100 in 0.1% sodium citrate) for 5 min on ice, and rinsed again twice with PBS. Next, 50 μl of TUNEL reaction mixture (from an in situ cell death detection kit; Boehringer-Mannheim) was added to the sample, and the Petri dishes were incubated in a humidified chamber for 60 min at 37 °C. Samples were either examined under a fluorescence microscope in this state, or under a phase-contrast microscope after signal conversion, which was accomplished by incubating samples with 50 μl of anti-fluorescein antibody conjugated with horseradish peroxidase (POD). The Petri dish was incubated in a humidified chamber for 60 min at 37 °C and rinsed with PBS. Finally, 50–100 μl of DAB substrate solution was added for 10 min at room temperature. The Petri dish was then rinsed with PBS and a glass coverslip was placed in the bottom of the dish, which was examined under a light microscope (Hong et al., 1998).

Cell counts

The number of TdT-dUTP-labeled nuclei (TUNEL-positive cells) and annexin V-fluorescein-positive cells in each sample was counted per 200 cells. Results were all expressed as mean ± SEM. Data were analyzed using either paired or unpaired Student's *t* tests, as appropriate. A value of $P < 0.05$ was taken to represent a statistically significant difference between group mean values.

Evaluation of mitochondrial membrane potential with a lipophilic cationic dye

For assessment of mitochondrial membrane potential ($\Delta\Psi$m), NNV-infected GL-av cells were stained using a MitoCapture (Mitochondria BioAssay™ Kit) that contained a lipophilic cation dye, which is trapped in mitochondria when $\Delta\Psi$m is normal and released into the cytoplasm when it is not. Loss of fluorescence intensity observed under fluorescence microscopy was taken as a marker of mitochondrial membrane potential disruption. GL-av cells were pretreated with 1.6 μM BKA or 40 μM CsA for 2 h before virus infection. The NNV-infected GL-av and normal control cells in 60-mm Petri dishes were incubated at 28 °C for 0, 24 h, and 48 h. Then, the medium was discarded, 500 μl of diluted MitoCapture reagent was added, and each dish was incubated at 37 °C for 15–20 min. Evaluation was by fluorescence microscopy using a 488-nm excitation and 515-nm long-pass filter for detection of fluorescein and using a 510-nm excitation and 590-nm long-pass filter for detection of rhodamine.

Quantification of cell viability

About 10^5 GL-av cells/ml were seeded in a 60-mm Petri dish, cultured for 20 h, and then pretreated with 1.6 μM BKA or 40 μM CsA for 2 h before virus infection. NNV-infected GL-av and normal control cells were incubated at 28 °C for 0, 24 h, and 48 h. At the completion of the various culture periods, the cell layers were washed with PBS, and treated with 0.5 ml of 0.1% trypsin-EDTA (GIBCO) 1−2 min. Cell viability was determined using a trypan blue dye exclusion assay (Mullen et al., 1975). Cell viability at each time point for each cell line was determined in triplicate; each point represents the mean viability of three independent experiments ± the standard error of the mean (SEM). Data were analyzed using either a paired or unpaired Student's *t* test as appropriate. A value of $P < 0.05$ was taken to represent a statistically significant difference between mean values of groups.

Staining secondary necrotic cells with acridine orange/ethidium bromide

One milliliter of cells (10^5 cells/ml of culture medium) was seeded into a 35-mm Petri dish (Nalge Nunc International) and incubated at 28 °C for 20 h. Cells were left untreated or were infected with 5 m.o.i. of virus and incubated for 0, 24 h, 48 h, or 72 h at 28 °C. At each time point, RGNNV-infected cells were stained with acridine orange (1 μg/ml)/ethidium bromide (1 μg/ml) in culture medium for 5 min at room temperature. The stained cells were placed on a glass slide and covered with a 22-mm^2 coverslip. To determine the proportion of dye-stained cells, Petri dishes were examined by fluorescence microscopy using an Olympus IX71 microscope equipped with a BP450-480 band-pass excitation filter and a BA515 barrier-emission filter.

Acknowledgments

The authors are grateful to Dr. H.L. Yang (Institute of Biotechnology, National Cheng-Kung University, Taiwan, ROC) for providing the grouper liver cell line (GL-a). This work was supported by grants (NSC-91-2311-B-006-007; NSC-92-2313-B-006-005) awarded to Dr. Jainn-Ruey Hong from the National Science Council, Taiwan, Republic of China.

References

Andree, H.A.M., Reutelingsperger, C.P.M., Hauptmann, R., Hemker, H.C., Hermens, W.T., Willems, G.M., 1990. Binding of vascular anticoagulant a (VACa) to planar phospholipids bilayers. J. Biol. Chem. 265, 4923–4928.

Ball, L.A., Johnson, K.L., 1999. Reverse genetics of nodaviruses. Adv. Virus Res. 53, 229–244.

Bauer, M.K.A., Schubert, A., Rocks, O., Grimm, S., 1999. Adenine nucleotide translocase-1, a component of the permeability transition pore, can dominantly induce apoptosis. J. Cell Biol. 147, 1493–1501.

Budd, S.L., Temet, L., Listnak, T., Lipton, S.A., 2000. Mitochondrial and extramitochondrial apoptotic signaling pathways in cerebrocortical neurons. Proc. Natl. Acad. Sci. U. S. A. 97, 6161–6166.

Chen, C.S., Huang, M., Marksich, S., Whitesides, G.M., Ingber, D.E., 1997. Genometric control of cell life and death. Science 276, 1425–1428.

Chipuk, J.E., Green, D.R., 2005. Do inducers of apoptosis trigger caspase-independent cell death? Nat. Rev., Mol. Cell Biol. 6, 268–275.

Compton, M., 1999. The mitochondria permeability transition pore and its role in cell death. Biochem. J. 341, 233–249.

Delsert, C., Morin, N., Comps, M., 1997. A fish encephalitis virus that differs from other nodaviruses by its capsid protein processing. Arch. Virol. 142, 2359–2371.

Duvall, E., Wyllie, A.H., 1986. Death and the cell. Immunol. Today 7, 115–119.

Fadok, V.A., Voelker, D.R., Campbell, P.A., Cohen, J.J., Bratton, D.L., Henson, P.M., 1992. Exposure of phosphatidylserine on the surface of apoptotic lymphocytes triggers specific recognition and removal by macrophages. J. Immunol. 148, 2207–2216.

Fadok, V.A., Bratton, D.L., Rose, D.M., Pearson, A., Ezekewitz, R.A., Henson, P.M., 2000. A receptor for phosphatidylserine-specific clearance of apoptotic cells. Nature 405, 85–90.

Falcieri, E., Gobbi, P., Zamai, L., Vitale, M., 1994. Ultrastructural features of apoptosis. Scanning Microsc. 8, 653–666.

Ferri, K.F., Kroemer, G., 2001. Organelle-specific initiation of cell death pathways. Nat. Cell Biol. 3, E255–E263.

Garzon, S., Strykowski, H., Charpentiter, G., 1990. Implication of mitochondria in the replication of Nodamura virus in larvae of the Lepidoptera, Galleria mellonella (L.) and in suckling mice. Arch. Virol. 113, 165–176.

Grotmol, S., Beerfh, O., Totland, G.K., 1999. Transmission of viral encephalopathy and retinopathy (VER) to yolk-sac larvae of the Atlantic halibut hippoglossus: occurrence of nodavirus in various organs and a possible route of infection. Dis. Aquat. Org. 36, 95–106.

Guo, Y.X., Wei, T., Dallmann, K., Kwang, J., 2003. Induction of caspase-dependent apoptosis by betanodaviruses GGNNV and demonstration of protein α as an apoptosis inducer. Virology 308, 74–82.

Guo, Y.X., Chan, S.W., Kwang, J., 2004. Membrane association of greasy grouper nervous necrosis virus protein A and characterization of its mitochondrial localization targeting signal. J. Virol. 78, 6498–6508.

Herman, B., Nieminen, A.L., Gores, G.J., Lemasters, J.J., 1988. Irreversible injury in anoxic hepatocytes precipitated by an abrupt increase in plasma membrane permeability. FASEB J. 2, 146–151.

Hong, J.R., Wu, J.L., 2002. Molecular regulation of cellular apoptosis by fish infectious pancreatic necrosis virus (IPNV) infection. Curr. Top. Virol. 2, 151–160.

Hong, J.R., Lin, T.L., Hsu, Y.L., Wu, J.L., 1998. Apoptosis proceeds necrosis of fish cell line by infectious pancreatic necrosis virus. Virology 250, 76–84.

Hong, J.R., Lin, G.H., Lin, C.J.F., Wang, W.P., Lee, C.C., Lin, T.L., Wu, J.L., 2004. Phosphatidylserine receptor is required for the engulfment of dead apoptotic cells and for normal embryonic development in zebrafish. Development 131, 5417–5427.

Inoue, Y., Yasukawa, M., Fujita, S., 1997. Induction of T-cell apoptosis by human herpesvirus 6. J. Virol. 71, 3751–3759.

Jaeschke, H., Lemasters, J.J., 2003. Apoptosis versus oncotic necrosis in hepatic ischemia/reperfusion injury. Gastroenterology 125, 1246–1257.

Jeurissen, S.H.M., Wagenaar, F., Pol, J.M.A., Vadereb, A.J., Noteborn, M.H. M., 1992. Chicken anemia virus causes apoptosis of thymocytes after in vivo infection and cell lines after in vitro infection. J. Virol. 66, 7383–7388.

Kain, S.R., Mai, K., Sinai, P., 1994. Human multiple tissue Western blots: a new immunological tool for the analysis of tissue-specific protein expression. BioTechniques 17, 982–987.

Kerr, J.F., Wyllie, A.H., Currie, A.R., 1972. Apoptosis: a basic biological phenomenon with wide-ranging implication in tissue kinetics. Br. J. Cancer 26, 239–257.

Kim, J.S., Qian, T., Lemasters, J.J., 2003. Mitochondrial permeability transition in the switch from necrotic to apoptotic cell death in ischemic rat hepatocytes. Gastroenterology 124, 494–503.

Koopman, G., Reutelingsperger, C.P.M., Kuijten, G.A.M., Keehnen, R.M.J., Pals, S.T., van Oers, M.H.J., 1994. Annexin V for flow cytometric detection of phosphatidylserine expression on B cells undergoing apoptosis. Blood 84, 1415–1420.

Kroemer, G., Martin, S.J., 2005. Caspase-independent cell death. Nat. Med. 11, 725–730.

Kroemer, G., Dallaporta, B., Resche-Rigon, M., 1998. The mitochondrial death/life regulator in apoptosis and necrosis. Annu. Rev. Physiol. 60, 619–642.

Kuwana, T., 1998. Apoptosis induction by caspase-8 is amplified through the mitochondrial release of cytochrome *c*. J. Biol. Chem. 273, 16589–16594.

Laemmli, U.K., 1970. Cleavage of structural proteins during the assembly of the head of bacteriophage T4. Nature 227, 680–685.

Lemasters, J.J., 1999. Necrapoptosis and the mitochondrial permeability transition: shared pathways to necrosis and apoptosis. Am. J. Physiol. 276, G1–G6.

Madesh, M., Antonsson, B., Srinivasula, S.M., Alnemri, E.S., Hajnoczky, G., 2002. Rapid kinetics of tBid-induced cytochrome *c* and Smac/DIABLO release and mitochondrial depolarization. J. Biol. Chem. 227, 5651–5659.

Majno, G., Joris, I., 1995. Apoptosis, oncosis and necrosis: an overview of cell death. Am. J. Pathol. 146, 3–15.

Martin, S.J., Reutelingsperger, C.P.M., McGahon, A.J., Rader, J., van Schie, R. C.C.A., LaFace, D., Green, D.R., 1995. Early redistribution of plasma membrane phosphatidylserine is a general feature of apoptosis regardless of the initiating stimulus: inhibition by overexpression of Bcl-2 and Abl. J. Exp. Med. 182, 1545–1556.

Marzo, I., Brenner, C., Zamzami, N., Jurgensmeier, J.M., Susin, S.A., L., Vieira, H., Prevost, M.C., Xie, Z., Matsuyama, S., Reed, J.C., 1998. Bax and adenine nucleotide translocator cooperate in mitochondrial control of apoptosis. Science 281, 2027–2031.

McConkey, D.J., Nicotera, P., Hartzell, P., Bellomo, G., Wyllie, A.H., Orrenius, S., 1989. Glucocorticoids activate a suicide process in thymocytes through an elevation of cytosolic Ca^{2+} concentration. Arch. Biochem. Biophys. 269, 365–370.

Miller, D.J., Schwartz, M.D., Ahlquist, P., 2001. Flock house virus RNA replicates on outer mitochondrial membranes in *Drosophila* cells. J. Virol. 75, 11664–11676.

Miller, D.J., Schwartz, M.D., Dye, B.T., Ahlquist, P., 2003. Engineered retargeting of viral RNA replication complexes to an alternative intracellular membrane. J. Virol. 77, 12193–12202.

Mori, K., Nakai, T., Muroga, K., Arimoto, M., Mushiake, K., Furusawa, I., 1992. Properties of a new virus belongs to Nodaviridae found in larval striped jack (*Pseudocaranx dentex*) with nervous necrosis. Virology 187, 368–371.

Mullen, P.D., Brand, R.J., Parlette, G.N., 1975. Evaluation of dye exclusion and colony inhibition techniques for detection of polyoma-specific, cell-mediated immunity. J. Natl. Cancer Inst. 54 (1), 229–231.

Nagai, T., Nishizawa, T., 1999. Sequence of the non-structural protein gene encoded by RNA1 of atriped jack nervous necrosis virus. J. Gen. Virol. 80, 3019–3022.

Nakai, T., Nguyen, H.D., Nishizawa, T., Muroga, K., Arimoto, M., Octsuki, K., 1994. Occurrence of viral nervous necrosis in kelp grouper and tiger puffer. Fish Pathol. 29, 211–212.

Narita, M., Shimizu, S., Ito, T., Chittenden, T., Leutz, R.J., Matsuda, H., Tsujimoto, Y., 1998. Bax interacts with the permeability transition pore to induce permeability transition and cytochrome *c* release in isolated mitochondria. Proc. Natl. Acad. Sci. U. S. A. 95, 14681–14686.

Newton, K., Strasser, A., 1998. The Bcl-2 family and cell death regulation. Curr. Opin. Genet. Dev. 8, 68–75.

Nieminen, A.L., Gores, G.J., Wray, B.E., Tanaka, Y., Herman, B., Lemasters, J. J., 1988. Calcium dependence of bleb formation and cell death in hepatocytes. Cell Calcium 9, 237–246.

Nishizawa, T., Mori, K., Furuhashi, M., Nakai, T., Furusawa, I., Muroga, K., 1995. Comparison of the coat protein genes of five fish nodaviruses, the causative agents of viral nervous necrosis in marine fish. J. Gen. Virol. 76, 1563–1569.

Raynal, P., Pollard, H.B., 1994. Annexins: the problem of assessing the biological role for a gene family of multifunctional calcium and phospholipids-binding proteins. Biochim. Biophys. Acta 1197, 63–93.

Savill, J., Fadok, V., 2000. Corpse clearance defines the meaning of cell death. Nature 407, 784–788.

Schneemann, A., Reddy, V., Johson, J.E., 1998. The structural and function of nodavirus particles: a paradigm for understanding chemical biology. Adv. Virus Res. 50, 381–446.

Shen, Y., Shenk, T.E., 1995. Viruses and apoptosis. Curr. Opin. Genet. Dev. 5, 105–111.

Shimizu, S., Narita, M., Tsujimoto, Y., 1999. Bcl-2 family proteins regulate the release of apoptogenic cytochrome *c* by the mitochondrial channel VDAC. Nature 399, 483–487.

Shimizu, S., Matsuoka, Y., Shinohara, Y., Yoneda, Y., Tsujimoto, Y., 2001. Essential role of voltage-dependent anion channel in various forms of apoptosis in mammalian cells. J. Cell Biol. 152, 237–250.

Sullivan, P.G., Thompson, M.B., Scheff, S.W., 1999. Cyclosporin A attenuates acute mitochondrial dysfunction following traumatic brain injury. Exp. Neurol. 160, 226–234.

Tafani, M., Schneider, T.G., Pastorino, J.G., Farber, J.L., 2000. Cytochrome *c*-dependent activation of caspase-3 by tumor necrosis factor requires induction of the mitochondrial permeability transition. Am. J. Pathol. 156, 2111–2121.

Tait, J.F., Gibson, D., Fujikawa, K., 1989. Phospholipid binding properties of human placental anticoagulant protein-1, a member of the lipoprotein family. J. Biol. Chem. 264, 7944–7949.

Thiagarajan, P., Tait, J.F., 1990. Binding of annexin V/placental anticoagulant protein to platelets: evidence for phosphatidylserine exposure in the procoagulant response of activated platelets. J. Biol. Chem. 265, 17420–17423.

Tyuriana, Y.Y., Tyurin, V.A., Zhao, Q., Djukic, M., Quinn, D.P., Pitt, B.R., Kagan, V.E., 2004. Oxidation of phosphatidylserine: a mechanism for plasma membrane phospholipids scrambling during apoptosis? Bioche. Biophy. Res. Commun. 324, 1059–1064.

Van Regenmorted, M.H.V., Fauquet, C.M., Bishop, D.H.L., Carstens, E.B., Estes, M.K., Lemon, S.M., McGeoch, D.J., Maniloff, J., Mayo, M.A., Pringle, C.R., Wickner, R.B., 2000. Virus Taxonomy. Seventh Report of the International Committee on Taxonomy of Viruses. Academic Press, San Diego.

Wang, X., 2001. The expanding role of mitochondria in apoptosis. Genes Dev. 15, 2922–2933.

Wyllie, A.H., 1980. Glucocorticoid-induced thymocyte apoptosis is associated with endogenous endonuclease activation. Nature 284, 555–556.

Wyllie, A.H., Kerr, J.F.R., Currie, A.R., 1980. Cell death: the significance of apoptosis. Int. Rev. Cytol. 68, 251–306.

Zamzami, N., Kroemer, G., 2001. The mitochondrion in apoptosis: how Pandora's box opens. Nat. Rev., Mol. Cell Biol. 2, 67–71.